Vertebrate Spt2 is a novel nucleolar histone chaperone that assists in ribosomal DNA transcription

Akihisa Osakabe[1], Hiroaki Tachiwana[1], Motoki Takaku[1], Tetsuya Hori[2], Chikashi Obuse[3], Hiroshi Kimura[4], Tatsuo Fukagawa[2,*] and Hitoshi Kurumizaka[1,*]

[1]Laboratory of Structural Biology, Graduate School of Advanced Science and Engineering, Waseda University, 2-2 Wakamatsu-cho, Shinjuku-ku, Tokyo 162-8480, Japan
[2]Department of Molecular Genetics, National Institute of Genetics and The Graduate University for Advanced Studies (SOKENDAI), Mishima, Shizuoka 411-8540, Japan
[3]Graduate School of Life Science, Hokkaido University, Kita-21, Nishi-11, Sapporo, Hokkaido 001-0021, Japan
[4]Graduate School of Frontier Biosciences, Osaka University, 1-3 Yamada-oka, Suita, Osaka 565-0871, Japan
*Authors for correspondence (kurumizaka@waseda.jp; tfukagaw@lab.nig.ac.jp)

Accepted 19 December 2012
Journal of Cell Science 126, 1323–1332

doi: 10.1242/jcs.112623

Summary

In eukaryotes, transcription occurs in the chromatin context with the assistance of histone-binding proteins, such as chromatin/nucleosome remodeling factors and histone chaperones. However, it is unclear how each remodeling factor or histone chaperone functions in transcription. Here, we identify a novel histone-binding protein, Spt2, in higher eukaryotes. Recombinant human Spt2 binds to histones and DNA, and promotes nucleosome assembly *in vitro*. Spt2 accumulates in nucleoli and interacts with RNA polymerase I in chicken DT40 cells, suggesting its involvement in ribosomal RNA transcription. Consistently, Spt2-deficient chicken DT40 cells are sensitive to RNA polymerase I inhibitors and exhibit decreased transcription activity, as shown by a transcription run-on assay. Domain analyses of Spt2 revealed that the C-terminal region, containing the region homologous to yeast Spt2, is responsible for histone binding, while the central region is essential for nucleolar localization and DNA binding. Based on these results, we conclude that vertebrate Spt2 is a novel histone chaperone with a separate DNA-binding domain that facilitates ribosomal DNA transcription through chromatin remodeling during transcription.

Key words: Histone chaperone, Nucleosome, Chromatin, Nucleoli, Transcription, RNA polymerase I

Introduction

In eukaryotes, genomic DNA is tightly packaged into chromatin, in which the four core histones, H2A, H2B, H3 and H4, form nucleosomes as the fundamental repeating unit of eukaryotic chromosomes (Wolffe, 1998). Nucleosomes cover almost the entire chromosome, including the promoters and coding regions of genes, and restrict the DNA binding of proteins that are required for transcription, replication, recombination, and repair of DNA in chromosomes. Therefore, nucleosomes are dynamically disassembled and reassembled with the aid of histone binding proteins, such as chromatin/nucleosome remodeling factors and histone chaperones, to facilitate the expression of genomic DNA.

Biochemical studies revealed that nucleosomes actually impede the initiation and elongation of transcription *in vitro* (Knezetic and Luse, 1986; Lorch et al., 1987; Izban and Luse, 1991). However, surprisingly, the rate of transcription elongation by RNA polymerase II in cells is about 1–4 kb/minute, which is roughly comparable to the rate of *in vitro* transcription with naked DNA (Singh and Padgett, 2009; Ardehali and Lis, 2009). This discrepancy may be reconciled by postulating the existence of chromatin/nucleosome remodeling factors, histone chaperones, and post-translational modifications of histones, which relieve the nucleosomal barrier in cells. Consistently, various chromatin/nucleosome remodeling factors and histone chaperones, together with histone modifications, have been identified, and their abilities to overcome the nucleosomal barrier during transcription have been characterized (Petesch and Lis, 2012). Chromatin/nucleosome remodeling factors and histone modifications are also required for RNA-polymerase-I-mediated ribosomal DNA (rDNA) transcription, probably to relieve the nucleosomal barrier in nucleoli (Chen and Pikaard, 1997; Percipalle et al., 2006; McStay and Grummt, 2008; Vintermist et al., 2011).

The major chromatin/nucleosome remodeling factors are composed of multiple protein complexes, and contain an ATP-hydrolyzing motor subunit as the active center for nucleosome eviction or sliding (Peterson, 2000; Alkhatib and Landry, 2011). Histone chaperones have been suggested to function with or without ATP-dependent chromatin and nucleosome remodeling factors during the assembly and disassembly of nucleosomes (Petesch and Lis, 2012). Unlike the major chromatin/nucleosome remodeling factors, histone chaperones do not require the energy of ATP hydrolysis (Avvakumov et al., 2011).

Among the histone chaperones, FACT (Orphanides et al., 1998; Belotserkovskaya et al., 2003; Saunders et al., 2003; Mason and Struhl, 2003) and Spt6 (Hartzog et al., 1998; Andrulis et al., 2000; Ardehali et al., 2009; Ivanovska et al., 2011) are known to associate with RNA polymerase II, and facilitate transcription elongation in chromatin. FACT also functions in

histone exchange during the repair of DNA double strand breaks (Heo et al., 2008). Another histone chaperone, Asf1, contributes to transcription processes (Schwabish and Struhl, 2006). These previous studies provided important insights for the functions of histone chaperones in the regulation of gene expression in cells. However, it is still unclear how each histone chaperone acts in transcription, because only a few histone chaperones that are directly involved in chromatin transcription have been reported so far.

To clarify the functional roles of histone-binding proteins, we performed a proteome analysis of histone binding proteins with HeLa cell extracts, and found several histone binding proteins, including an acidic histone chaperone, sNASP (Osakabe et al., 2010). In this study, we describe the functions of a novel histone-binding protein, Spt2. Human Spt2 contains a short region homologous to *Saccharomyces cerevisiae* Spt2 (Spt2-like motif) in its C-terminus (Winston et al., 1984; Sternberg et al., 1987). Biochemical analyses revealed that human Spt2 possesses histone binding, DNA binding, and nucleosome assembly activities *in vitro*. In addition, we demonstrated that Spt2 accumulates in nucleoli, and interacts with RNA polymerase I in chicken DT40 cells. To examine the function of Spt2 *in vivo*, we created Spt2-deficient DT40 cells, which exhibited higher sensitivity to reagents that inhibit RNA polymerase I transcription. In addition, the rate of transcription was markedly decreased in the Spt2-deficient DT40 cells, based on a run-on assay. Considering these results, we concluded that vertebrate Spt2 is a novel histone chaperone that functions in chromatin dynamics during the RNA-polymerase-I-dependent transcription processes in nucleoli.

Results

Identification of human Spt2 as a histone-binding protein

To identify the proteins interacting with the histone H3/H4 complex, we prepared Affi-gel 10 beads conjugated with the H3/H4 complex, and the human proteins bound to the H3/H4 beads were isolated from the HeLa cell extracts and analyzed by high-sensitivity mass spectrometry. In both the cytoplasmic and chromatin fractions of the cell extracts, we detected several known histone-binding proteins, including MCM2, MCM4, MCM6, MCM7 (Ishimi et al., 1996), SUPT16H (Spt16; FACT140) (Orphanides et al., 1998), SSRP1 (FACT80) (Orphanides et al., 1998), SUPT6H (Spt6) (Bortvin and Winston, 1996), and NASP (Wang et al., 2008; Osakabe et al., 2010). MCM2-4-6-7 is a subcomplex of the MCM2-7 hexamer, which functions as a helicase in replication initiation (Bochman and Schwacha, 2009). SUPT16H and SSRP1 form the FACT complex, which functions as a histone chaperone during transcription, replication and repair (Winkler and Luger, 2011). SUPT6H and NASP are also known as histone chaperones that directly bind to core histones (Bortvin and Winston, 1996; Wang et al., 2008; Osakabe et al., 2010). Thus, our pull-down experiments with the H3/H4 beads were proved to be useful to identify histone-binding proteins in HeLa cell extracts.

Among the various potential histone-binding proteins, we found a protein that encodes a product of the human *SPTY2D1* gene (NCBI: 144108). This protein is basic (pI=9.79) and composed of 685 amino acid residues, with a short sequence homologous to the *S. cerevisiae* Spt2 protein (Spt2-like domain) in the C-terminal region (Fig. 1A). Since we did not find any other known motifs in this protein and any other proteins harboring the Spt2-like domain in the human protein database, we refer to this protein as hsSpt2. Mutations of yeast Spt2 suppress the mutations caused by Ty and δ insertions in the 5′ non-coding region of the HIS4 gene locus (Winston et al., 1984). Additional analyses suggested that yeast Spt2 may function in the remodeling and/or maintenance of chromatin structure during transcription (Peterson et al., 1991; Nourani et al., 2006; Thebault et al., 2011).

Spt2-like domain of hsSpt2 is responsible for histone binding

To investigate the function of hsSpt2, we expressed and purified hsSpt2 as a recombinant protein (Fig. 1A,B) and tested its histone-binding activity. Purified hsSpt2 was incubated with either the histone H3/H4 complex or the histone H2A/H2B complex, and complex formation was analyzed by 5% non-denaturing PAGE and Coomassie Brilliant Blue staining. As shown in Fig. 1C,D, hsSpt2 binds to both the H2A/H2B and H3/H4 complexes. To identify the histone-binding domain of hsSpt2, we prepared two hsSpt2 deletion mutants, hsSpt2(1-570) and hsSpt2(571-685) (Fig. 1A,B). hsSpt2(571-685) contains the acidic Spt2-like domain (Fig. 1A). We performed a pull-down assay, using the Ni-NTA beads with the His_6-tagged H3/H4 complex. As shown in Fig. 1E, full-length hsSpt2 was efficiently captured by the Ni-NTA beads in the presence of His_6-tagged H3/H4 (lane 4), but not in the absence of His_6-tagged H3/H4 (lane 3). Our pull-down assay revealed that hsSpt2(571-685) efficiently bound to H3/H4, but hsSpt2(1-570) barely did so (Fig. 1E, lanes 7 and 10). These results indicated that the acidic Spt2-like domain is responsible for H3/H4 binding.

hsSpt2 preferentially binds to branched DNA

We next analyzed the DNA-binding activity of hsSpt2 with various kinds of DNA. For this experiment, we prepared Holliday junction DNA, Y-form DNA, and double-stranded DNA, by annealing oligonucleotides (Iwasaki et al., 1992) and purifying them by native PAGE (Horikoshi et al., 2010). Each of these specifically structured DNAs and single-stranded DNAs was incubated with hsSpt2, and the DNA–protein complexes were analyzed by 8% non-denaturing PAGE and SYBR Gold staining. As shown in Fig. 2A, hsSpt2 bound to single-stranded, double-stranded, Y-form and Holliday junction DNA. A competitive DNA-binding experiment revealed that hsSpt2 preferentially bound to branched DNAs (i.e. the Y-form and Holliday junction DNAs), over single-stranded and double-stranded DNA (Fig. 2B,C). Interestingly, hsSpt2(1-570), which lacked the Spt2-like domain, was completely proficient in the DNA-binding activity and preferred branched DNAs (Fig. 2D, lanes 1–10). In contrast, hsSpt2(571-685) did not bind to the DNAs (Fig. 2D, lanes 11–15). Therefore, we concluded that the acidic Spt2-like domain binds to histones, but is not involved in DNA binding.

hsSpt2 has nucleosome assembly activity

The histone-binding and DNA-binding activities of hsSpt2 prompted us to test its nucleosome assembly activity. Nucleosome assembly can be assessed by the increased number of negative supercoils on DNA, when nucleosomes are formed on closed circular DNA in the presence of topoisomerase I (Osakabe et al., 2010) (Fig. 3A). hsSpt2 significantly induced supercoils into closed circular DNA in the presence of histones H2A, H2B,

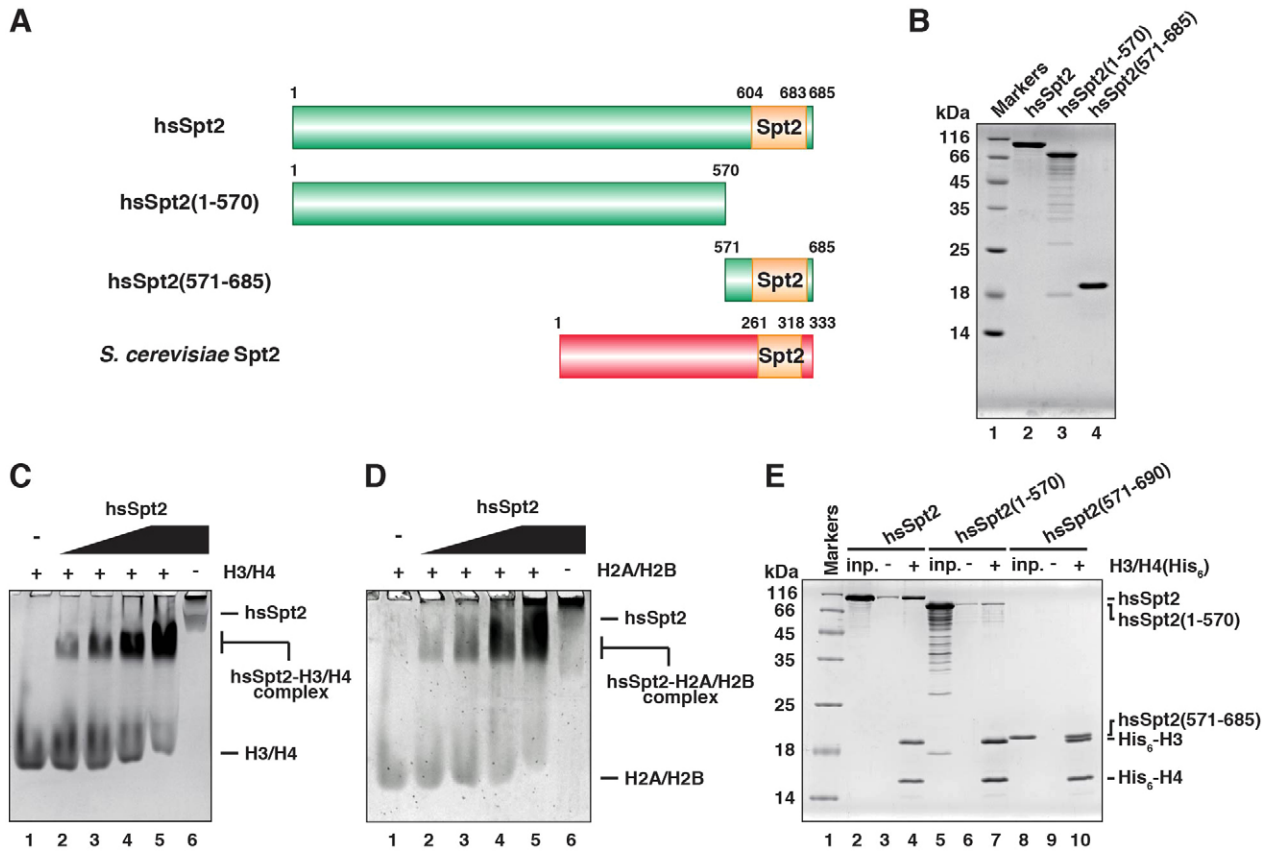

Fig. 1. Purification and histone-binding activity of hsSpt2. (**A**) Representations of hsSpt2, hsSpt2(1-570), hsSpt2(571-685) and *S. cerevisiae* Spt2. Boxes denoted as Spt2 represent regions corresponding to the Spt2-like motif. The numbers indicate amino acid residues. (**B**) Purification of hsSpt2, hsSpt2(1-570) and hsSpt2(571-685). SDS-PAGE analysis of purified hsSpt2 (lane 2), hsSpt2(1-570) (lane 3), and hsSpt2(571-685) (lane 4) lacking the His_6 tag. Lane 1 indicates molecular mass markers. Note that the purified hsSpt2(1-570) preparation contained many degradation products, as compared with the full-length hsSpt2, indicating that the lack of the Spt2-like domain destabilizes hsSpt2. (**C**) hsSpt2 binds to the H3/H4 complex. H3/H4 (13.4 μM, 3.6 μg) was mixed with various amounts of hsSpt2 (lanes 2–6). The samples were incubated for 1 hour at 23℃ and then fractionated by 5% non-denaturing PAGE in 0.5× TBE buffer. The bands were visualized by Coomassie Brilliant Blue staining. The amounts of hsSpt2 were 0 μM (lane 1), 0.38 μM (lane 2), 0.75 μM (lane 3), 1.5 μM (lane 4) and 3 μM (lanes 5 and 6). (**D**) hsSpt2 binds to the H2A/H2B complex. H2A/H2B (12.6 μM, 3.6 μg) was mixed with various amounts of hsSpt2 (lanes 2–6). The experimental procedure was the same as for C. The amounts of hsSpt2 were 0 μM (lane 1), 0.38 μM (lane 2), 0.75 μM (lane 3), 1.5 μM (lane 4) and 3 μM (lanes 5 and 6). (**E**) Pull-down assay with Ni-NTA beads. Lane 1 represents molecular mass markers. Lanes 2–4, 5–7 and 8–10 indicate experiments with hsSpt2, hsSpt2(1-570) and hsSpt2(571-685), respectively. Lanes 2, 5 and 8 represent 25% of input proteins. Lanes 3, 6 and 9 indicate negative control experiments without His_6-tagged H3/H4. Lanes 4, 7 and 10 indicate experiments with His_6-tagged H3/H4. The proteins bound to His_6-tagged H3/H4 were captured by the Ni–NTA agarose beads. The samples were fractionated by 18% SDS-PAGE, and were visualized by Coomassie Brilliant Blue staining.

H3, and H4, in a dose-dependent manner (Fig. 3B, lanes 4–6). In contrast, hsSpt2 alone in the absence of histones did not induce supercoils into the DNA (Fig. 3B, lane 7). Based on these results, we concluded that hsSpt2 possesses nucleosome-assembly activity *in vitro*.

Spt2-deficient DT40 cells are sensitive to actinomycin D and mitomycin C, which covalently bind to DNA and inhibit RNA polymerase

To clarify the function of Spt2, we created Spt2-deficient chicken DT40 cells and characterized their phenotype. Chicken Spt2 (ggSpt2) shares significant sequence homology with hsSpt2 over the entire protein (supplementary material Fig. S1A). We created gene disruption constructs to replace exons 3–4 of the ggSpt2 gene with drug resistance genes (supplementary material Fig. S1B), and sequentially introduced these constructs into DT40 cells. We disrupted both alleles of the ggSpt2 gene in DT40 cells by homologous recombination (supplementary material Fig. S1C), and two clones with the *ggSpt2*−/− allele were obtained (supplementary material Fig. S1B–D). We found that ggSpt2 is not essential for cell viability, since the *ggSpt2*−/− cells grew normally under standard culture conditions (Fig. 4A; supplementary material Fig. S2A).

However, the Spt2-deficient DT40 cells exhibited severe growth defects, as compared to the wild-type cells, in the presence of 10 nM actinomycin D (a selective inhibitor of RNA polymerase I at <100 nM; Perry and Kelley, 1970) and 7.5 nM mitomycin C (a potent DNA crosslinking agent), but not 100 nM hydroxyurea (a DNA synthesis inhibitor) or 80 nM anisomycin (a protein synthesis inhibitor) (Fig. 4). The cell mortality by apoptosis significantly increased in the presence of either actinomycin D or mitomycin C (supplementary material Fig. S2B,C; Fig. S3). The sensitivity to the low concentration of actinomycin D is consistent with the possible function of Spt2 in rDNA transcription. Although mitomycin C is known to preferentially crosslink the CG sequence and inhibit DNA

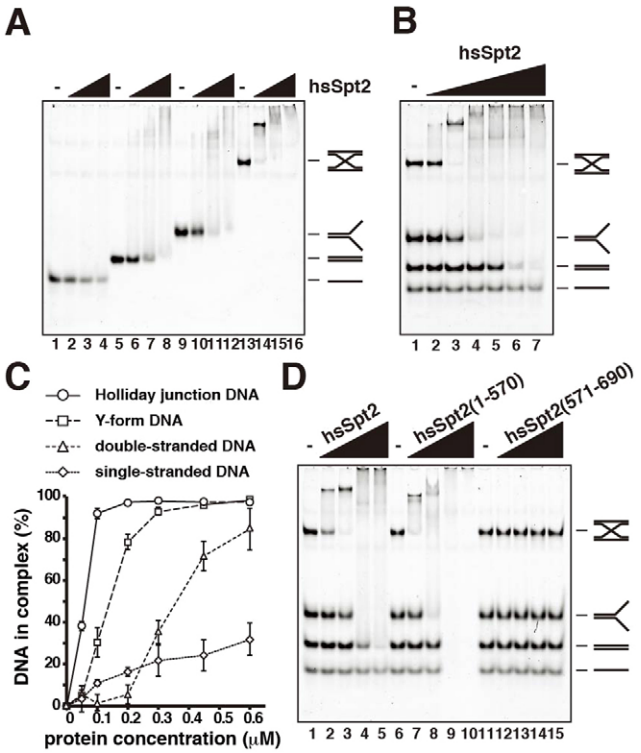

Fig. 2. DNA-binding activity of hsSpt2. (**A**) hsSpt2 binds single-stranded DNA, double-stranded DNA, Y-form DNA and Holliday junction DNA. Each DNA substrate (3 μM) was incubated with hsSpt2 at 37℃ for 15 minutes. The samples were then fractionated on an 8% non-denaturing polyacrylamide gel in 0.5× TBE buffer. The hsSpt2 concentrations were 0 μM (lanes 1, 5, 9 and 13), 0.1 μM (lanes 2, 6, 10 and 14), 0.2 μM (lanes 3, 7, 11 and 15), and 0.3 μM (lanes 4, 8, 12 and 16). The DNA and its complexes were visualized by SYBR Gold staining. (**B**) Competitive DNA binding experiments with single-stranded DNA, double-stranded DNA, Y-form DNA and Holliday junction DNA. Increasing amounts of hsSpt2 were incubated with the DNA mixture, containing the four DNA substrates (3 μM each), at 37℃ for 15 minutes. The hsSpt2 concentrations were 0 μM (lane 1), 0.05 μM (lane 2), 0.1 μM (lane 3), 0.2 μM (lane 4), 0.3 μM (lane 5), 0.45 μM (lane 6) and 0.6 μM (lane 7). The samples were fractionated by electrophoresis on an 8% non-denaturing polyacrylamide gel in 0.5× TBE buffer, and visualized by SYBR Gold staining. (**C**) Graphic representation of the experiments shown in B. The amounts of the complexes formed were estimated from the residual free DNA substrates. Averages of three independent experiments are presented with the standard deviation values. (**D**) Competitive DNA binding experiments for hsSpt2(1-570) and hsSpt2(571-685) with single-stranded DNA, double-stranded DNA, Y-form DNA, and Holliday junction DNA. Increasing amounts of hsSpt2, hsSpt2(1-570) or hsSpt2(571-685) were incubated with the DNA mixture, containing the four DNA substrates (3 μM each) at 37℃ for 15 minutes. The hsSpt2, hsSpt2(1-570) or hsSpt2(571-685) concentrations were 0 μM (lanes 1, 6 and 11), 0.05 μM (lanes 2, 7 and 12), 0.1 μM (lanes 3, 8 and 13), 0.3 μM (lanes 4, 9 and 14) and 0.4 μM (lanes 5, 10 and 15). The samples were fractionated by electrophoresis on an 8% non-denaturing polyacrylamide gel in 0.5× TBE buffer, and visualized by SYBR Gold staining.

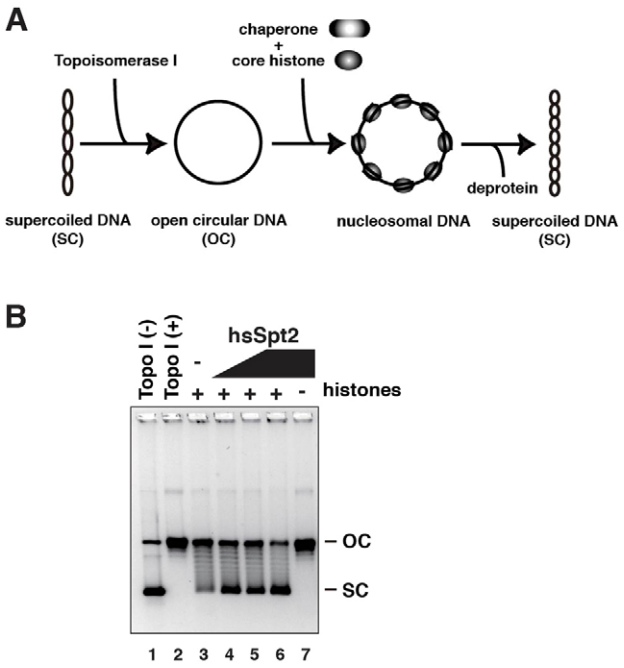

Fig. 3. Nucleosome assembly activity of hsSpt2. (**A**) Representation of the supercoiling assay. (**B**) Open circular φX174 DNA (10 ng/μl), prepared by wheat germ topoisomerase I treatment (lane 2), was incubated with hsSpt2 (lanes 4–6) in the presence of core histones. The reaction products were analyzed by 1% agarose gel electrophoresis in 1× TAE buffer. Lanes 3 and 7 indicate negative control experiments without hsSpt2 in the presence of core histones and without core histones in the presence of hsSpt2, respectively. The amounts of hsSpt2 were 0 μM (lanes 1–3), 0.1 μM (lane 4), 0.2 μM (lane 5) and 0.4 μM (lanes 6 and 7).

synthesis, it also inhibits rDNA transcription (Snodgrass et al., 2010). Consistently, we found that ggSpt2 was localized to nucleoli in DT40 cells (Fig. 5A). Co-immunoprecipitation assays with an anti-Spt2 polyclonal antibody revealed that ggSpt2 interacted with endogenous histone H3 and RNA polymerase I (Fig. 5B). The phenotype of the Spt2-deficient cells, combined with the localization and co-immunoprecipitation data, strongly supports the idea that vertebrate Spt2 functions during transcription processes in nucleoli.

Central region of Spt2 is largely responsible for targeting to nucleoli

GFP-fused ggSpt2 significantly accumulated in DT40 nucleoli (Fig. 5A). We then expressed ten different ggSPT2 deletion mutants as GFP-fused proteins in DT40 cells, and examined their localizations (Fig. 6; supplementary material Fig. S4). Interestingly, ggSpt2(1-576), lacking the Spt2-like domain, efficiently localized in nucleoli (Fig. 6A,C), indicating that the Spt2-like domain is not required for the nucleolar localization, although it is essential for histone binding (Fig. 1E). In contrast, ggSpt2(577-690), containing only the Spt2-like domain, did not accumulate in nucleoli (Fig. 6B,C). These data indicated that the histone binding domain is separated from the nucleolar targeting domain.

To obtain further domain information, we tested eight other deletion mutants. For the C-terminally deleted mutants, ggSpt2(1-412) and ggSpt2(1-311) accumulated in nucleoli with 2-fold higher signal intensities, as compared to the other nuclear regions (Fig. 6C; supplementary material Fig. S4B,C). However, ggSpt2(1-192) and ggSpt2(1-100) did not specifically accumulate in nucleoli (Fig. 6C; supplementary material Fig. S4D,E). For the N-terminally deleted mutants, no clear nucleolar accumulation was observed with ggSpt2(413-690) (Fig. 6C; supplementary material Fig. S4F) and ggSpt2(577-690) (Fig. 6B,C), and

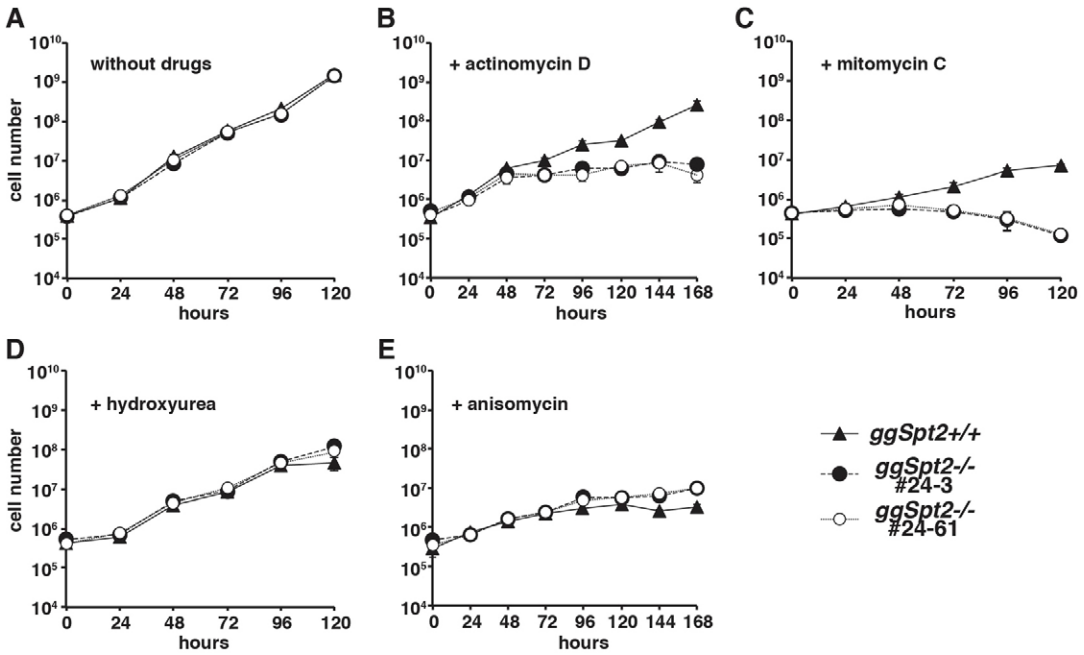

Fig. 4. Growth curves of wild-type and *ggSpt2−/−* DT40 cells in the presence or absence of drug. (**A**–**E**) Wild-type (closed triangles) and *ggSpt2−/−* DT40 cells (clones no. 24-3 and no. 24-61; closed circles and open circles, respectively) were plated ($4\sim5\times10^5$ cells/vial) and grown in medium without drugs (A), or containing 10 nM actinomycin D (B), 7.5 nM mitomycin C (C), 100 nM hydroxyurea (D) and 10 nM anisomycin (E). The number of cells, excluding cells stained by Trypan Blue, was counted every 24 hours ($n=3$).

moderate nucleolar accumulation was detected with ggSpt2(312-690) (Fig. 6C; supplementary material Fig. S4G). In contrast, ggSpt2(193-690) and ggSpt2(101-690) clearly accumulated in nucleoli (Fig. 6C; supplementary material Fig. S3H,I). Considering these localization data, we concluded that the region including amino acid residues 193–412 of ggSpt2 is largely responsible for targeting to nucleoli.

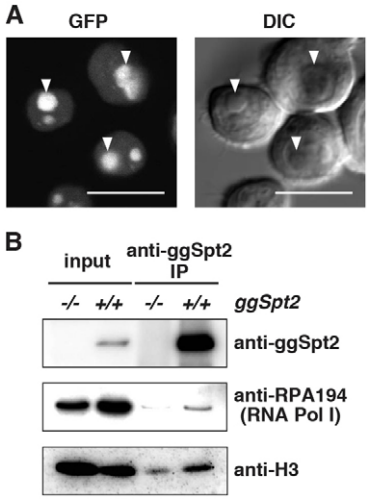

Fig. 5. Nucleolar localization of ggSpt2. (**A**) ggSpt2 is localized in nucleoli. GFP-fused ggSpt2 was expressed in *ggSpt2−/−* DT40 cells and visualized in the living cells. The fluorescent (left) and differential interference contrast (right) images were obtained using a confocal microscope (IX-71; Olympus) with a 100× oil-immersion objective lens. Scale bars: 10 μm.
(**B**) Immunoprecipitation of ggSpt2. The wild-type and *ggSpt2−/−* DT40 cells (6×10^8 cells) were collected and sonicated. After centrifugation, the supernatants were incubated with Protein G Sepharose 4 beads coupled with anti-ggSpt2, and the proteins associated with ggSpt2 were precipitated. The samples (×125 input) were then fractionated by SDS-PAGE, and the proteins detected by their respective antibodies.

Transcriptional activity is impaired in Spt2-deficient cells

We next performed a transcription run-on assay, to directly address whether vertebrate Spt2 is involved in transcription. In this assay, the cells were permeabilized, and the engaged RNA polymerases were allowed to continue transcription in the presence of ^{32}P-labeled nucleotides. The radioactivity in the acid-insoluble RNA was then measured. We found that the amounts of transcripts generated by the run-on reaction were significantly reduced in the Spt2-deficient DT40 cells, as compared to wild-type cells (Fig. 7A; supplementary material Fig. S5A). Importantly, the exogenous expression of ggSpt2 in the Spt2-deficient DT40 cells restored the transcription rate to the wild-type level (Fig. 7A), indicating that Spt2 is actually involved in the transcription process in cells.

To determine how the Spt2 deficiency caused the transcription reduction, we performed run-on assays in the presence various RNA polymerase inhibitors. As compared to the wild type cells, the transcription reduction was still observed in the Spt2-deficient cells in the presence of 10 μg/ml α-amanitin (RNA polymerase II and III inhibitor; Fig. 7B; supplementary material Fig. S5B). In contrast, the transcription levels were similar in the wild-type and Spt2-deficient cells in the presence of 80 nM actinomycin D (RNA polymerase I inhibitor; supplementary material Fig. S5C). These data indicated that Spt2 functions in RNA-polymerase-I-mediated transcription.

We next tested whether the DNA- and histone-binding activities of Spt2 are required for the RNA-polymerase-I-mediated

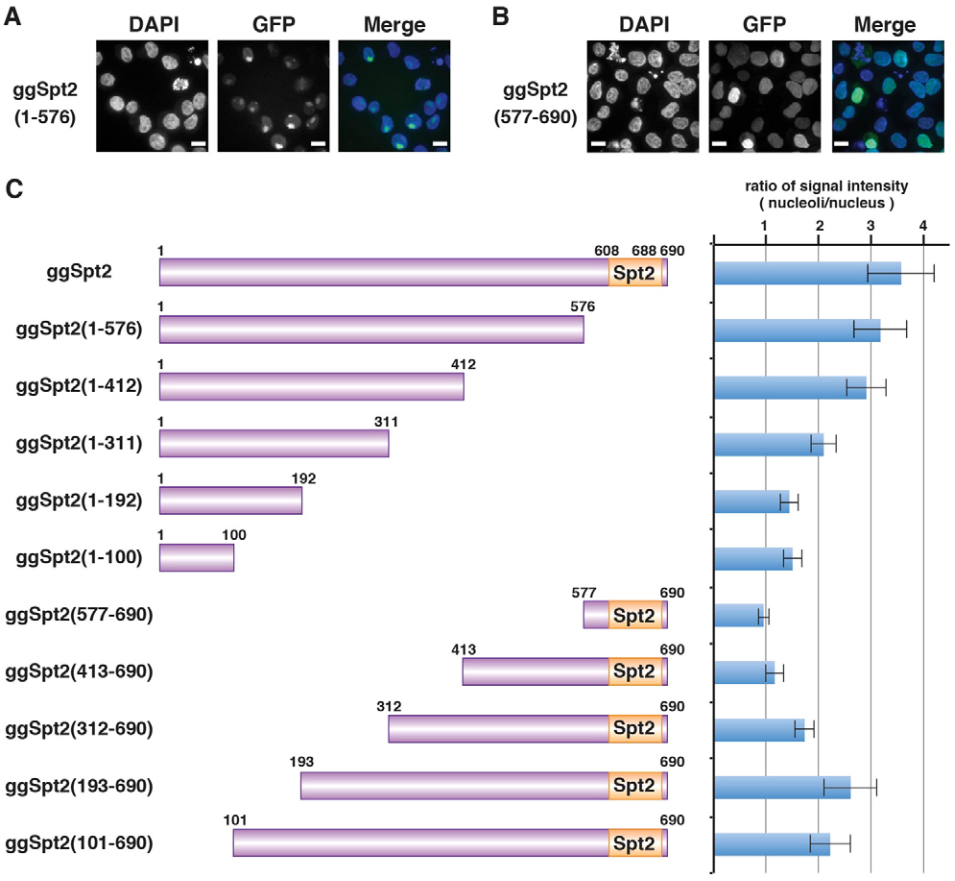

Fig. 6. Mapping of the nucleolar targeting domain of ggSpt2. (**A**,**B**) GFP-fused ggSpt2(1-576) (A) or ggSpt2(577-690) (B) were expressed in the *ggSpt2*−/− DT40 cells. DNA was visualized by DAPI staining (blue). Scale bars: 10 μm. (**C**) Graphic representation of the nucleolar targeting activities of the ggSpt2 deletion mutants. The names of the ggSpt2 deletion mutants are indicated on the left. Ratios of GFP signal intensity in nucleoli relative to other nuclear regions are plotted with standard deviation values (n=50).

transcription. We performed the run-on assays with Spt2-deficient cells expressing either ggSpt2(1-576; defective in histone binding) or ggSpt2(577-690; defective in DNA binding) (Figs 1, 2). As shown in Fig. 7C, neither ggSpt2(1-576) nor ggSpt2(577-690) restored the transcription to the normal level in the Spt2-deficient cells, suggesting that both the histone-binding and DNA-binding activities are required for the function assisting in RNA polymerase I transcription. In conclusion, Spt2 localizes to nucleoli, and is involved in facilitating proper transcription by RNA polymerase I. Although the histone-binding domain is not involved in nucleolar localization, it is required for transcription.

Discussion

In eukaryotes, histone-binding proteins perform multiple functions in the regulation of genomic DNA, such as replication, repair, recombination, and transcription, to relieve

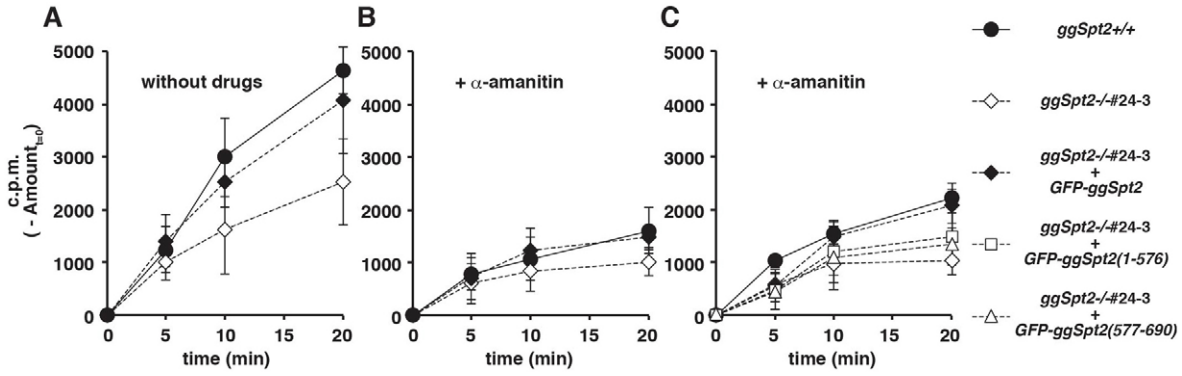

Fig. 7. Reduced transcription in the Spt2-deficient cells. (**A**–**C**) Run-on assay. The cells (1.5×10^7 cells) were collected and permeabilized. After washing, cells were incubated at 30℃ (0, 5, 15 or 20 minutes) with 40 μM each of ATP, GTP, UTP, CTP and [α-^{32}P]UTP and 160 μM $MgCl_2$, in the presence (B,C) or absence (A) of 10 μg/ml α-amanitin. After the incubation, aliquots of the cells were spotted on GF/C filters, which were washed with 5% trichloroacetic acid and rinsed with 70% ethanol. The amounts of [^{32}P]RNA on the GF/C filter were measured with a scintillation counter. Closed circles represent the positive control experiments with wild-type cells. Open diamonds indicate *ggSpt2*−/− DT40 cells. Closed diamonds, open squares and open triangles indicate the cell lines that express GFP-fused ggSpt2, ggSpt2(1-576) and ggSpt2(577-690) in *ggSpt2*−/− DT40 cells, respectively. Means ± s.d. are shown (n=3).

the inhibitory effects of nucleosomes. Extensive studies on the abilities of RNA polymerases to surmount nucleosomes have been performed (Clark and Felsenfeld, 1992; Studitsky et al., 1994; Studitsky et al., 1995; Studitsky et al., 1997; Bondarenko et al., 2006). Chromatin/nucleosome remodeling factors and histone chaperones have been identified as the machinery that relieves the nucleosome barrier during transcription processes (Petesch and Lis, 2012). Chromatin and nucleosome remodeling factors actively promote nucleosome sliding, using energy from ATP hydrolysis (Peterson, 2000; Alkhatib and Landry, 2011). In contrast, histone chaperones are usually acidic, and passively function in the nucleosome assembly and disassembly processes by binding to basic histones, without the energy of ATP hydrolysis (Avvakumov et al., 2011). The members of this ATP-independent nucleosome assembly/disassembly family are emerging as essential players in gene expression. However, it is still unclear how each nucleosome assembly/disassembly factor acts in transcriptional regulation.

In this study, we found the novel vertebrate histone-binding protein Spt2, which promotes nucleosome assembly *in vitro*. Unlike the known acidic histone chaperones, hsSpt2 is basic (pI=9.79). However, our deletion analysis revealed that the region encompassing the C-terminal 115 amino acid residues (containing the Spt2-like domain), which is acidic (pI=4.71), is responsible for the histone-binding activity of hsSpt2, suggesting that the histone-binding mechanism of hsSpt2 may be similar to that of other acidic histone chaperones.

In our proteome analyses of histone binding proteins, we also identified known acidic histone chaperones, including NASP, NAP1L1 (Nap1), and NAP1L4 (Nap2); however, these acidic histone chaperones were predominantly found in the cytoplasmic fraction. These findings are consistent with the idea that 'histone chaperones' may not be stably incorporated into chromatin. In contrast, hsSpt2 was present only in the chromatin fraction. Interestingly, we found that the Spt2-like domain, which is responsible for histone binding, is not required for both the DNA-binding and nucleolar-targeting activities, suggesting that the nucleolar (chromatin) targeting of Spt2 depends on its DNA-binding activity, but not on its histone-binding activity. Among the different forms of DNA tested, hsSpt2 binds preferentially to branched DNAs, such as the Y-form and Holliday junction DNAs, which may be correlated with the enrichment of cruciform/Holliday-structured DNA in nucleoli (Ward et al., 1991). The acidic histone chaperones usually lack DNA-binding activity. Therefore, hsSpt2 is a unique histone chaperone with a separate DNA-binding domain.

We found that Spt2 interacts with RNA polymerase I, and that the Spt2-deficient DT40 cells are sensitive to the RNA polymerase I inhibitors actinomycin D and mitomycin C. In addition, the rate of transcription governed by RNA polymerase I is clearly decreased in the Spt2-deficient DT40 cells, as compared to wild-type cells. These *in vivo* results suggested that vertebrate Spt2 functions with active RNA polymerase I, in a manner reminiscent of the yeast *S. cerevisiae* Spt2 (scSpt2), which genetically interacts with RNA polymerase II (Peterson et al., 1991). The DNA binding and nucleolar targeting domains in vertebrates may have been acquired during evolution, and the functions may have become specialized to rDNA transcription. scSpt2 reportedly functions with transcription elongation factors, in addition to RNA polymerase (Nourani et al., 2006). Genome-wide chromatin immunoprecipitation experiments revealed that scSpt2 is predominantly associated with the coding regions of genes, and promotes nucleosome assembly in a transcription-dependent manner, probably behind the transcribing RNA polymerase (Nourani et al., 2006; Thebault et al., 2011). Therefore, vertebrate Spt2 may share some functions with yeast Spt2, although the sequence similarity between yeast Spt2 and vertebrate Spt2 is restricted.

Nucleoli contain clusters of rDNA repeats. Nucleosomes are largely depleted from the rDNA coding sequences, due to robust transcription by RNA polymerase I (French et al., 2003), but are present on the intergene sequence (IGS) and internal transcription spacer regions between the coding sequences of rDNAs (Zentner et al., 2011). In yeast, however, the coding region of the rDNA is fully covered by nucleosomes (Jones et al., 2007). Even if the coding region of rDNA lacks nucleosomes, the dynamic balance of nucleosome assembly and disassembly may still be important in the initiation and/or elongation of transcription in nucleoli. Spt2 may bind to naked DNA to promote the assembly and/or disassembly of nucleosomes on rDNA. The reduced rate of RNA polymerase I transcription in Spt2-knockout DT40 cells suggested that Spt2 may play a positive role in rDNA transcription, by removing nucleosomes in front of a polymerase and/or assembling them behind it. Although nucleosomes generally reduce the transcription rate, the transient assembly of nucleosomes behind a polymerase may regulate the torsional stress of DNA or prevent damage to naked DNA, which may in turn facilitate transcription. Consistently, Spt2-knockout DT40 cells show higher sensitivity to DNA intercalating and crosslinking reagents (actinomycin D and mitomycin C), which stall RNA polymerase.

Alternatively, the transcription-coupled nucleosome assembly activity may function to regulate the number of transcriptionally active rDNAs, by establishing the transcriptionally repressed chromatin structure after RNA polymerase passage on the rDNA repeats. Consistent with this idea, the number of active and repressed rDNAs is constantly balanced in nucleoli (Conconi et al., 1989; French et al., 2003; Strohner et al., 2004; Santoro and Grummt, 2005). In this context, the DNA-binding activity of Spt2 may be required to promote nucleosome assembly on the naked DNA region behind an active RNA polymerase, in a similar manner to the histone H3.3-specific chaperone HIRA complex, which may directly bind to naked DNA and associate with an active RNA polymerase (Ray-Gallet et al., 2011).

So far, two nucleolar histone chaperones have been reported in mammals: B23/Nucleophosmin/numatrin/NPM1 (Okuwaki et al., 2001) and nucleolin (Angelov et al., 2006). In addition, yeast FKBP has been shown to possess histone chaperone activity and regulate ribosomal gene silencing (Kuzuhara and Horikoshi, 2004; Xiao et al., 2006). These three nucleolar proteins can be classified into a group of acidic histone chaperones. The features of Spt2 differ from those of the acidic histone chaperones, because it is a basic protein, it directly binds to DNA through a distinct domain other than the Spt2-like chaperone domain, and it binds to RNA polymerase I. Therefore, we believe that vertebrate Spt2 is a representative of a new class of nucleolar histone chaperones, which associate with chromatin by their DNA-binding activity and function as nucleosome assembly/disassembly factors in the regulation of rDNA transcription.

Materials and Methods

Purification of recombinant hsSpt2 and deletion mutants hsSpt2(1-570) and hsSpt2(571-690)

The DNA fragment encoding hsSpt2, hsSpt2(1-570), or hsSpt2(571-685) was ligated into the *Nde*I and *Bam*HI sites of the pET15b vector (Novagen), in which the thrombin protease recognition sequence was replaced by the PreScission protease recognition sequence (GE Healthcare Biosciences). Freshly transformed *E. coli* BL21(DE3) cells, bearing the hsSpt2, hsSpt2(1-570), or hsSpt2(571-685) expression vector and an expression vector for the minor tRNAs (Codon(+)RP; Stratagene), were grown on LB plates containing ampicillin (100 μg/ml) and chloramphenicol (35 μg/ml) at 37℃. After a 16-hour incubation, 5–20 colonies on the LB plates were collected and inoculated into LB medium (10 l) containing ampicillin (100 μg/ml) and chloramphenicol (35 μg/ml), and the cultures were incubated at 30℃. When the cell density reached an OD_{600}=0.4, 0.5 mM isopropyl-β-D-thiogalactopyranoside was added to induce the expression of hsSpt2, hsSpt2(1-570), or hsSpt2(571-685) as the N-terminally His_6 tagged protein [His_6-hsSpt2, His_6-hsSpt2(1-570), or His_6-hsSpt2(571-685)], and the cultures were further incubated at 18℃ for 12 hours. The cells producing His_6-hsSpt2 were harvested, resuspended in 50 mM Tris-HCl buffer (pH 8.0), containing 2 mM 2-mercaptoethanol, 10% glycerol, and 500 mM NaCl, and disrupted by sonication. The cells producing His_6-hsSpt2(1-570) or His_6-hsSpt2(571-685) were harvested, resuspended in 50 mM Tris-HCl buffer (pH 8.0), containing 2 mM 2-mercaptoethanol, 10% glycerol, 0.05% Nonidet P-40, and 500 mM NaCl, and disrupted by sonication. The cell debris was removed by centrifugation (27,216×***g***; 20 minutes), and the lysate was mixed gently with 4 ml (50% slurry) of nickel-nitrilotriacetic acid (Ni-NTA) agarose resin (Qiagen) at 4℃ for 1 hour. The Ni-NTA beads bound to His_6-hsSpt2, His_6-hsSpt2(1-570), or His_6-hsSpt2(571-685) were then packed into an Econo-column (Bio-Rad), and washed with 100 ml of 50 mM Tris-HCl buffer (pH 8.0), containing 10% glycerol, 500 mM NaCl, 5 mM imidazole, and 2 mM 2-mercaptoethanol, at a flow rate of about 1 ml/minute. His_6-hsSpt2, His_6-hsSpt2(1-570), or His_6-hsSpt2(571-685) was eluted by a 100 ml linear gradient of imidazole from 5 to 500 mM in 50 mM Tris-HCl buffer (pH 8.0), containing 10% glycerol, 500 mM NaCl, and 2 mM 2-mercaptoethanol. The fractions containing His_6-hsSpt2, His_6-hsSpt2(1-570), or His_6-hsSpt2(571-685) were diluted with the same volume of 50 mM Tris-HCl buffer (pH 8.0), containing 10% glycerol and 2 mM 2-mercaptoethanol, and were loaded on a 3 ml hydroxyapatite column (Bio-Rad) at 4℃. The column containing His_6-hsSpt2 was then washed with 90 ml of 60 mM sodium phosphate (pH 7.9), containing 250 mM NaCl, 1 mM EDTA, 10% glycerol, and 2 mM 2-mercaptoethanol. His_6-hsSpt2 was then eluted by a 100 ml linear gradient of 250–300 mM NaCl and 60–200 mM sodium phosphate (pH 7.9). The column containing His_6-hsSpt2(1-570) or His_6-hsSpt2(571-685) was washed with 90 ml of 5 mM sodium phosphate (pH 8.0), containing 250 mM NaCl, 1 mM EDTA, 10% glycerol, and 2 mM 2-mercaptoethanol. His_6-hsSpt2(1-570) or His_6-hsSpt2(571-685) was then eluted by a 100 ml linear gradient of 250–350 mM NaCl and 5–150 mM sodium phosphate (pH 8.0). The His_6 tag was removed from the hsSpt2 portion by PreScission protease [5 units/mg for hsSpt2, 3 units/mg for hsSpt2(1-570) and His_6-hsSpt2(571-685)]. The sample was immediately dialyzed against 20 mM Tris-HCl buffer (pH 8.0), containing 200 mM NaCl, 1 mM EDTA, 10% glycerol, and 2 mM 2-mercaptoethanol. After removing the His_6 tag, hsSpt2 was further purified by MonoS (GE Healthcare Biosciences) column chromatography, with elution by a 30 ml linear gradient of 200–600 mM NaCl in 20 mM Tris-HCl buffer (pH 8.0), containing 1 mM EDTA, 10% glycerol, and 2 mM 2-mercaptoethanol. The peak fractions were collected and dialyzed against 20 mM Tris-HCl buffer (pH 8.0), containing 200 mM NaCl, 1 mM EDTA, 10% glycerol, and 2 mM 2-mercaptoethanol. After dialysis, hsSpt2 was further purified by MonoQ (GE Healthcare Biosciences) column chromatography, with elution by a 10 ml linear gradient of 200–600 mM NaCl in 20 mM Tris-HCl buffer (pH 8.0), containing 1 mM EDTA, 10% glycerol, and 2 mM 2-mercaptoethanol. On the other hand, hsSpt2(1-570) was loaded onto a MonoQ column, and the flow through fraction was collected. The MonoQ flow through fraction of hsSpt2(1-570) was further purified by MonoS column chromatography, with elution by a 20 ml linear gradient of 200–600 mM NaCl in 20 mM Tris-HCl buffer (pH 8.0), containing 1 mM EDTA, 10% glycerol, and 2 mM 2-mercaptoethanol. hsSpt2(571-685) was loaded onto a MonoS column, and the flow through fraction was collected. The MonoS flow through fraction was further purified by MonoQ column chromatography, with elution by a 10 ml linear gradient of 200–600 mM NaCl in 20 mM Tris-HCl buffer (pH 8.0), containing 1 mM EDTA, 10% glycerol, and 2 mM 2-mercaptoethanol. The purified hsSpt2, hsSpt2(1-570), and hsSpt2(571-685) proteins were dialyzed against 20 mM Tris-HCl buffer (pH 8.0), containing 200 mM NaCl, 0.1 mM EDTA, 10% glycerol, and 2 mM 2-mercaptoethanol, and the hsSpt2 concentration was determined by densitometric analysis of the Coomassie Brilliant-Blue-stained SDS-PAGE gel, using BSA (Pierce Biotechnology) as the standard protein.

Preparation of recombinant human histones

Human H2A, H2B, H3.1, and H4 were overexpressed in *Escherichia coli* cells as N-terminal His_6-tagged proteins (Tanaka et al., 2004), and were purified by the method described previously (Tachiwana et al., 2010). The H3.1/H4 complex was reconstituted as follows. H3.1 was combined with H4 at a 1:1 molar ratio in 20 mM Tris-HCl (pH 7.5) buffer, containing 7 M guanidine hydrochloride and 20 mM 2-mercaptoethanol, and the mixture was dialyzed overnight against 20 mM Tris-HCl (pH 7.5) buffer, containing 1 mM EDTA, 1 mM PMSF, 5% glycerol, 5 mM 2-mercaptoethanol, and 2 M NaCl. The NaCl concentration was then reduced by stepwise dialysis at 4℃: 1 M NaCl for 4 hours, 0.5 M NaCl for 4 hours, and 0.1 M NaCl overnight. The H2A/H2B complex was also reconstituted by the same method. The reconstituted H3.1/H4 and H2A/H2B complexes were fractionated on Superdex 200 resin (GE Healthcare Biosciences) packed in an Econo-column (1.6×13.5 cm; 0.5 ml/minute flow rate; 0.5 ml fractions) with 20 mM Tris-HCl (pH 7.5) buffer, containing 1 mM EDTA, 1 mM PMSF, 5% glycerol, 0.1 M NaCl, and 5 mM 2-mercaptoethanol.

Assay for histone binding by hsSpt2 (native polyacrylamide gel assay)

H3.1/H4 (13.4 μM, 3.6 μg) or H2A/H2B (12.6 μM, 3.6 μg) was mixed with hsSpt2 (0.38–3 μM, 0.28–2.27 μg) in 10 μl of 20 mM Tris-HCl buffer (pH 8.0), containing 140 mM NaCl and 1 mM dithiothreitol. The samples were then incubated for 1 hour at 23℃. After the incubation, the samples were fractionated by 5% non-denaturing PAGE in 0.5× TBE buffer (45 mM Tris base, 45 mM boric acid, and 1 mM EDTA). The electrodes were conversely connected, and the samples were electrophoresed at 10.4 V/cm. The bands were visualized by Coomassie Brilliant Blue staining.

Gel electrophoretic mobility shift assay for DNA binding by hsSpt2, hsSpt2(1-570) and hsSpt2(571-685)

To analyze the DNA binding activities of hsSpt2, hsSpt2(1-570), and hsSpt2(571-685), we prepared Holliday junction DNA, Y-form DNA, double-stranded DNA, and single-stranded DNA from oligonucleotides. The Holliday junction DNA was prepared by annealing four 49-mer single-stranded oligonucleotides (1), (2), (3), and (4), with the sequences (1) 5′-ATCGATGTCTCTAGACAGCTGC-TCAGGATTGATCTGTAATGGCCTGGGA-3′, (2) 5′-GTCCCAGGCCATTAC-AGATCAATCCTGAGCATGTTTACCAAGCGCATTG-3′, (3) 5′-TGATCACT-TGCTAGCGTCGCAATCCTGAGCAGCTGTCTAGAGACATCGA-3′, and (4) 5′-CCAATGCGCTTGGTAAACATGCTCAGGATTGCGACGCTAGCAAGTG-ATC-3′. The Holliday junction DNA contained a 12 base-pair homologous region at its center, and each 5′ end of the four strands contained a one base overhang. The Y-form DNA (a 30-bp duplex region and two 18 base and 19 base single strands) was prepared by annealing oligonucleotides (1) and (2). The double-stranded DNA was prepared by annealing oligonucleotide (2) with its complementary oligonucleotide. Oligonucleotide (2) was used as the single-stranded DNA. All oligonucleotides used in this study were purified by HPLC, and the DNA concentrations are expressed as moles of nucleotides.

In the DNA-binding assay, the single-stranded DNA (3 μM), the double-stranded DNA (3 μM), the Y-form DNA (3 μM), and the Holliday junction DNA (3 μM) were incubated with the indicated amounts of hsSpt2, hsSpt2(1-570), or hsSpt2(571-685) at 37℃ for 15 minutes, in 10 μl of 20 mM Tris-HCl buffer (pH 8.0), containing 1 mM $MgCl_2$, 0.1 mg/ml BSA, and 1 mM dithiothreitol. For competitive DNA-binding assays, the indicated amounts of hsSpt2, hsSpt2(1-570), or hsSpt2(571-685) were incubated with the mixture of the single-stranded DNA (3 μM), the double-stranded DNA (3 μM), the Y-form DNA (3 μM), and the Holliday junction DNA (3 μM) at 37℃ for 15 minutes, in 10 μl of 20 mM Tris-HCl buffer (pH 8.0), containing 1 mM $MgCl_2$, 0.1 mg/ml BSA, and 1 mM dithiothreitol. The products were analyzed by 8% non-denaturing PAGE in 0.5× TBE buffer at 6.25 V/cm for 2 hours, and were visualized by SYBR Gold (Invitrogen) staining.

Ni-NTA bead pull-down assay

Purified His_6-tagged H3.1/H4 (200 pmol) was mixed with hsSpt2, hsSpt2(1-570), or hsSpt2(571-685) (200 pmol) in 500 μl of 20 mM Tris-HCl buffer (pH 8.0), containing 150 mM NaCl and 15 mM imidazole. The Ni-NTA agarose beads (3 μl, 50% slurry) were added to the reaction mixture, and the samples were then incubated for 1 hour at 4℃ with rotation. After the incubation, the Ni-NTA agarose beads with His_6-tagged H3.1/H4 were pelleted and washed three times with 500 μl of 20 mM Tris-HCl buffer (pH 8.0), containing 200 mM NaCl, 30 mM imidazole, and 0.2% Tween 20. The proteins captured by the Ni-NTA agarose beads were analyzed by SDS-18% PAGE. The bands were visualized by CBB staining.

Supercoiling assay for nucleosome assembly

The supercoiling assay (topological assay) was performed according to the method described previously (Osakabe et al., 2010). H2A/H2B (10 ng/μl) and H3.1/H4 (10 ng/μl) were preincubated with the indicated amounts of hsSpt2 at 37℃ for 15 min. To initiate the reaction, relaxed ϕX174 DNA (10 ng/μl), prepared by an incubation with 1.7 U wheat germ topoisomerase I (Promega) per 100 ng DNA at 37℃ for 150 minutes, was added to the reaction mixture, and the reactions were continued in 10 μl of 20 mM Tris-HCl buffer (pH 8.0), containing 140 mM NaCl,

2 mM $MgCl_2$, and 5 mM DTT, at 37℃ for 60 minutes. The samples were then incubated at 42℃ for 60 minutes, and the proteins were removed by an incubation with 60 µl of a proteinase K solution (20 mM Tris-HCl (pH 8.0), 20 mM EDTA, 0.5% SDS, and 0.5 mg/ml proteinase K) at 37℃ for 15 minutes, followed by phenol-chloroform extraction. The DNA samples were then analyzed by 1% agarose gel electrophoresis in 1× TAE buffer (40 mM Tris acetate and 1 mM EDTA) at 3.3 V/cm for 4 hours, and were visualized by SYBR Gold (Invitrogen) staining.

Establishment of ggSpt2-deficient DT40 cells

DT40 cells were cultured and transfected as described previously (Buerstedde and Takeda, 1991). The amplified ggSpt2 cDNA was used as a probe to isolate genomic DNA clones specific for ggSpt2 from a DT40 genomic DNA library. The genomic DNA clone containing the ggSpt2-coding region was cloned into pBluescript (Stratagene). The ggSpt2 disruption construct was then inserted into the histidinol or puromycin resistance vector, under the control of the β-actin promoter. To select the ggSpt2-disrupted cells, the growth medium was supplemented with histidinol (2 mg/ml, Sigma-Aldrich) and puromycin (0.5 µg/ml, Clontech). The ggSpt2 gene disruption was confirmed by a Southern blot analysis of genomic DNA.

Western blot analysis for ggSpt2-deficient DT40 cells

The *ggSpt2*+/+ and *ggSpt2*−/− DT40 cells were collected and lysed in 2× SDS gel loading buffer. The samples were fractionated by 12% SDS-PAGE and transferred to a Hybond-P PVDF membrane (GE Healthcare), using a semi-dry blotting system (BIO CRAFT). The membrane was washed with TBS-T (20 mM Tris-HCl (pH 7.5), 137 mM NaCl, and 0.1% Tween 20), and was blocked with TBS-T containing 0.5% skimmed milk (Nacalai Tesque), followed by washing with TBS-T. The membrane was incubated at room temperature with anti-ggSpt2 (301-690) antisera (1:500) in TBS-T, and then washed three times in TBS-T. The peptide containing amino acid residues 301–690 of ggSpt2, which are highly conserved between ggSpt2 and hsSpt2, was used as the antigen for the ggSpt2 antisera. The membrane was then incubated with peroxidase-conjugated anti-rabbit Ig (1:6000; GE Healthcare) in TBS-T, and washed three times with TBS-T. Signals were developed using ECL Western Blotting Detection Reagents (GE Healthcare) and detected using an LAS-4000 image analyzer (Fujifilm).

Sensitivities of the Spt2-deficient DT40 cells to drug treatments

The *ggSpt2*+/+ and *ggSpt2*−/− DT40 cells were cultured in medium, containing 100 nM hydroxyurea (Sigma-Aldrich), 80 nM anisomycin (Sigma-Aldrich), 7.5 nM mitomycin C (Kyowa Hakko Kirin), or 10 nM actinomycin D (Sigma-Aldrich). To measure the cell density, the cells were mixed with a Trypan Blue solution (Invitrogen), and the number of live cells excluding the dye was counted.

Cell cycle analysis of ggSpt2-deficient DT40 cells

The *ggSpt2*+/+ and *ggSpt2*−/− DT40 cells were cultured in medium containing 7.5 nM mitomycin C or 10 nM actinomycin D for 48 hours, and were pulse-labeled with 20 µM BrdU (Roche) for 20 minutes. The cells were harvested and fixed at −30℃ with 70% ethanol. The cells were then washed with PBS containing 1% BSA, and were treated with 4 M HCl in 0.5% Triton X-100 for 30 minutes. After washing with PBS containing 1% BSA, the cells were incubated with an anti-BrdU antibody (Becton Dickinson) for 1 hour, followed by an incubation with fluorescein isothiocyanate (FITC)-conjugated anti-mouse IgG (Jackson ImmunoResearch Laboratories) for 30 minutes. The cells were then stained with 10 µg/ml propidium iodide (Sigma) in PBS containing 1% BSA. Flow cytometry was performed with an Epics Altra cytometer (Beckman-Coulter). Fluorescence data were displayed as dot plots by the Altra analysis software (Beckman-Coulter).

TUNEL assay

The cells were cultured in medium containing 7.5 nM mitomycin C for 48 hours, harvested, washed with PBS, and fixed in 3% paraformaldehyde for 20 minutes. After the fixed cells were washed with PBS, they were treated with a solution containing 0.1% Na-citrate and 0.1% Triton X-100, on ice. The cells were washed with PBS, and a terminal deoxynucleotidyltransferase-mediated dUTP-biotin nick end labeling (TUNEL) reaction was performed, according to the manufacturer's protocol (*in situ* cell death detection kit, fluorescein; Roche). The stained cells were washed with PBS, and then stained with 10 ng/ml DAPI. The fluorescent images were obtained using a confocal microscope (IX-71; Olympus) with a 100× oil-immersion objective lens.

Subnuclear localization analysis of ggSpt2

The Spt2-deficient DT40 cells, expressing GFP-ggSpt2, were plated on a glass-bottom dish. The fluorescent images were obtained using a confocal microscope (FV-1000; Olympus) with a 60× PlanApo N (NA=1.4) oil-immersion objective lens, as previously described (Hayashi-Takanaka et al., 2011).

Immunoprecipitation assay with ggSpt2

Cultured *ggSpt2*+/+ and *ggSpt2*−/− DT40 cells (6×10^8 cells) were collected and washed with sonication buffer [50 mM HEPES-NaOH (pH 7.4), 150 mM NaCl, 10% glycerol, 1 mM EDTA, 0.5% NP-40, 0.25% Triton X-100, and protease inhibitors (Complete, Roche)]. The cells were resuspended in sonication buffer (1×10^8 cells/ml) and sonicated. The samples were centrifuged, and the supernatants were incubated overnight with anti-ggSpt2 antibody-conjugated Protein G Sepharose 4 Fast Flow resin (GE Healthcare Biosciences) at 4℃. The beads were then washed with sonication buffer, and the proteins (×125 input) were fractionated by 5–20% SDS-PAGE (Wako). The proteins in the gels were transferred to a Hybond-P PVDF membrane, using a semi-dry blotting system (Bio-Rad). The PVDF membrane was probed with rabbit anti-ggSpt2 (1:1000), mouse anti-RPA194 (1:500; F-6, Santa Cruz Biotechnology, Inc.), and rat anti-H3 (1:3000) antibodies.

Nucleolar localization analyses for GFP-ggSpt2 deletion mutants

The DNA sequences encoding the ggSpt2 deletion mutants, ggSpt2(1-576), ggSpt2(1-412), ggSpt2(1-311), ggSpt2(1-192), ggSpt2(1-100), ggSpt2(577-690), ggSpt2(413-690), ggSpt2(312-690), ggSpt2(193-690), and ggSpt2(101-690), composed of amino acid residues 1–576, 1–412, 1–311, 1–192, 1–100, 577–690, 413–690, 312–690, 193–690 and 101–690 of ggSpt2, respectively, were ligated into the pEGFP-C1 vector (Clontech). These plasmids were transfected into the *ggSpt2*−/− DT40 cells, and G418 (final concentration of 2 mg/ml, Sigma) was added to select for stable transfectants. The cells expressing each ggSpt2 deletion mutant were fixed with paraformaldehyde, and were stained with 10 ng/ml DAPI. The fluorescent images were collected using a confocal microscope (IX-71; Olympus) with a 100× oil-immersion objective lens, and the signal intensities were analyzed with the ImageJ software (National Institutes of Health).

Run-on assay

The transcription run-on analysis was performed as previously described (Kimura et al., 1999), with some optimizing modifications for DT40 cells. The *ggSpt2*+/+ cells (1.5×10^7 cells), *ggSpt2*−/− cells (1.5×10^7 cells), and *ggSpt2*−/− cells expressing GFP-ggSpt2 or its deletion mutants (1.5×10^7 cells) were collected and washed with PBF (100 mM CH_3COOK, 30 mM KCl, 10 mM Na_2HPO_4, 1 mM $MgCl_2$, 1 mM ATP, 1 mM DTT, and 5% Ficoll). The cells were permeabilized with PBF containing 100 µg/ml digitonin for 5 minutes on ice, and were washed with PBF. The cells were then incubated at 30℃ (for 0, 5, 15, or 20 minutes) in PBF containing ATP (40 µM), GTP (40 µM), UTP (40 µM), CTP (40 µM), [α-^{32}P]UTP (PerkinElmer; at a final concentration of 0.74 MBq/ml), and 160 µM $MgCl_2$, in the absence or presence of 10 µg/ml α-amanitin or 80 nM actinomycin D. After the incubation, aliquots of the cells were spotted on GF/C filters (Whatman), which were washed with 5% trichloroacetic acid and rinsed with 70% ethanol. The amounts of [^{32}P]RNA on the GF/C filters were measured with a scintillation counter.

Author contributions

A.O., H.T., and M.T. purified hsSpt2 and histones, and performed biochemical analyses. A.O., T.H., H. Kimura, and T.F. performed the cell biological experiments. A.O. and C.O. performed the proteome analysis of the histone binding proteins. H. Kurumizaka and T.F. conceived, designed, and supervised all of the work. A.O., H. Kimura, T.F. and H. Kurumizaka wrote the paper. All of the authors discussed the results and commented on the manuscript.

Funding

This work was supported in part by Grants-in-Aid from the Japanese Society for the Promotion of Science (JSPS) and the Ministry of Education, Culture, Sports, Science and Technology (MEXT), Japan. H.K. is supported as a research fellow in the Waseda Research Institute for Science and Engineering.

Supplementary material available online at
http://jcs.biologists.org/lookup/suppl/doi:10.1242/jcs.112623/-/DC1

References

Alkhatib, S. G. and Landry, J. W. (2011). The nucleosome remodeling factor. *FEBS Lett.* **585**, 3197-3207.

Andrulis, E. D., Guzmán, E., Döring, P., Werner, J. and Lis, J. T. (2000). High-resolution localization of Drosophila Spt5 and Spt6 at heat shock genes in vivo: roles in promoter proximal pausing and transcription elongation. *Genes Dev.* **14**, 2635-2649.

Angelov, D., Bondarenko, V. A., Almagro, S., Menoni, H., Mongélard, F., Hans, F., Mietton, F., Studitsky, V. M., Hamiche, A., Dimitrov, S. et al. (2006). Nucleolin is

a histone chaperone with FACT-like activity and assists remodeling of nucleosomes. *EMBO J.* **25**, 1669-1679.

Ardehali, M. B. and Lis, J. T. (2009). Tracking rates of transcription and splicing in vivo. *Nat. Struct. Mol. Biol.* **16**, 1123-1124.

Ardehali, M. B., Yao, J., Adelman, K., Fuda, N. J., Petesch, S. J., Webb, W. W. and Lis, J. T. (2009). Spt6 enhances the elongation rate of RNA polymerase II in vivo. *EMBO J.* **28**, 1067-1077.

Avvakumov, N., Nourani, A. and Côté, J. (2011). Histone chaperones: modulators of chromatin marks. *Mol. Cell* **41**, 502-514.

Belotserkovskaya, R., Oh, S., Bondarenko, V. A., Orphanides, G., Studitsky, V. M. and Reinberg, D. (2003). FACT facilitates transcription-dependent nucleosome alteration. *Science* **301**, 1090-1093.

Bochman, M. L. and Schwacha, A. (2009). The Mcm complex: unwinding the mechanism of a replicative helicase. *Microbiol. Mol. Biol. Rev.* **73**, 652-683.

Bondarenko, V. A., Steele, L. M., Ujvári, A., Gaykalova, D. A., Kulaeva, O. I., Polikanov, Y. S., Luse, D. S. and Studitsky, V. M. (2006). Nucleosomes can form a polar barrier to transcript elongation by RNA polymerase II. *Mol. Cell* **24**, 469-479.

Bortvin, A. and Winston, F. (1996). Evidence that Spt6p controls chromatin structure by a direct interaction with histones. *Science* **272**, 1473-1476.

Buerstedde, J. M. and Takeda, S. (1991). Increased ratio of targeted to random integration after transfection of chicken B cell lines. *Cell* **67**, 179-188.

Chen, Z. J. and Pikaard, C. S. (1997). Epigenetic silencing of RNA polymerase I transcription: a role for DNA methylation and histone modification in nucleolar dominance. *Genes Dev.* **11**, 2124-2136.

Clark, D. J. and Felsenfeld, G. (1992). A nucleosome core is transferred out of the path of a transcribing polymerase. *Cell* **71**, 11-22.

Conconi, A., Widmer, R. M., Koller, T. and Sogo, J. M. (1989). Two different chromatin structures coexist in ribosomal RNA genes throughout the cell cycle. *Cell* **57**, 753-761.

French, S. L., Osheim, Y. N., Cioci, F., Nomura, M. and Beyer, A. L. (2003). In exponentially growing Saccharomyces cerevisiae cells, rRNA synthesis is determined by the summed RNA polymerase I loading rate rather than by the number of active genes. *Mol. Cell. Biol.* **23**, 1558-1568.

Hartzog, G. A., Wada, T., Handa, H. and Winston, F. (1998). Evidence that Spt4, Spt5, and Spt6 control transcription elongation by RNA polymerase II in Saccharomyces cerevisiae. *Genes Dev.* **12**, 357-369.

Hayashi-Takanaka, Y., Yamagata, K., Wakayama, T., Stasevich, T. J., Kainuma, T., Tsurimoto, T., Tachibana, M., Shinkai, Y., Kurumizaka, H., Nozaki, N. et al. (2011). Tracking epigenetic histone modifications in single cells using Fab-based live endogenous modification labeling. *Nucleic Acids Res.* **39**, 6475-6488.

Heo, K., Kim, H., Choi, S. H., Choi, J., Kim, K., Gu, J., Lieber, M. R., Yang, A. S. and An, W. (2008). FACT-mediated exchange of histone variant H2AX regulated by phosphorylation of H2AX and ADP-ribosylation of Spt16. *Mol. Cell* **30**, 86-97.

Horikoshi, N., Morozumi, Y., Takaku, M., Takizawa, Y. and Kurumizaka, H. (2010). Holliday junction-binding activity of human SPF45. *Genes Cells* **15**, 373-383.

Ishimi, Y., Ichinose, S., Omori, A., Sato, K. and Kimura, H. (1996). Binding of human minichromosome maintenance proteins with histone H3. *J. Biol. Chem.* **271**, 24115-24122.

Ivanovska, I., Jacques, P. E., Rando, O. J., Robert, F. and Winston, F. (2011). Control of chromatin structure by spt6: different consequences in coding and regulatory regions. *Mol. Cell. Biol.* **31**, 531-541.

Iwasaki, H., Takahagi, M., Nakata, A. and Shinagawa, H. (1992). Escherichia coli RuvA and RuvB proteins specifically interact with Holliday junctions and promote branch migration. *Genes Dev.* **6**, 2214-2220.

Izban, M. G. and Luse, D. S. (1991). Transcription on nucleosomal templates by RNA polymerase II in vitro: inhibition of elongation with enhancement of sequence-specific pausing. *Genes Dev.* **5**, 683-696.

Jones, H. S., Kawauchi, J., Braglia, P., Alen, C. M., Kent, N. A. and Proudfoot, N. J. (2007). RNA polymerase I in yeast transcribes dynamic nucleosomal rDNA. *Nat. Struct. Mol. Biol.* **14**, 123-130.

Kimura, H., Tao, Y., Roeder, R. G. and Cook, P. R. (1999). Quantitation of RNA polymerase II and its transcription factors in an HeLa cell: little soluble holoenzyme but significant amounts of polymerases attached to the nuclear substructure. *Mol. Cell. Biol.* **19**, 5383-5392.

Knezetic, J. A. and Luse, D. S. (1986). The presence of nucleosomes on a DNA template prevents initiation by RNA polymerase II in vitro. *Cell* **45**, 95-104.

Kuzuhara, T. and Horikoshi, M. (2004). A nuclear FK506-binding protein is a histone chaperone regulating rDNA silencing. *Nat. Struct. Mol. Biol.* **11**, 275-283.

Lorch, Y., LaPointe, J. W. and Kornberg, R. D. (1987). Nucleosomes inhibit the initiation of transcription but allow chain elongation with the displacement of histones. *Cell* **49**, 203-210.

Mason, P. B. and Struhl, K. (2003). The FACT complex travels with elongating RNA polymerase II and is important for the fidelity of transcriptional initiation in vivo. *Mol. Cell. Biol.* **23**, 8323-8333.

McStay, B. and Grummt, I. (2008). The epigenetics of rRNA genes: from molecular to chromosome biology. *Annu. Rev. Cell Dev. Biol.* **24**, 131-157.

Nourani, A., Robert, F. and Winston, F. (2006). Evidence that Spt2/Sin1, an HMG-like factor, plays roles in transcription elongation, chromatin structure, and genome stability in Saccharomyces cerevisiae. *Mol. Cell. Biol.* **26**, 1496-1509.

Okuwaki, M., Matsumoto, K., Tsujimoto, M. and Nagata, K. (2001). Function of nucleophosmin/B23, a nucleolar acidic protein, as a histone chaperone. *FEBS Lett.* **506**, 272-276.

Orphanides, G., LeRoy, G., Chang, C. H., Luse, D. S. and Reinberg, D. (1998). FACT, a factor that facilitates transcript elongation through nucleosomes. *Cell* **92**, 105-116.

Osakabe, A., Tachiwana, H., Matsunaga, T., Shiga, T., Nozawa, R. S., Obuse, C. and Kurumizaka, H. (2010). Nucleosome formation activity of human somatic nuclear autoantigenic sperm protein (sNASP). *J. Biol. Chem.* **285**, 11913-11921.

Percipalle, P., Fomproix, N., Cavellán, E., Voit, R., Reimer, G., Krüger, T., Thyberg, J., Scheer, U., Grummt, I. and Farrants, A. K. (2006). The chromatin remodelling complex WSTF-SNF2h interacts with nuclear myosin 1 and has a role in RNA polymerase I transcription. *EMBO Rep.* **7**, 525-530.

Perry, R. P. and Kelley, D. E. (1970). Inhibition of RNA synthesis by actinomycin D: characteristic dose-response of different RNA species. *J. Cell. Physiol.* **76**, 127-139.

Peterson, C. L. (2000). ATP-dependent chromatin remodeling: going mobile. *FEBS Lett.* **476**, 68-72.

Peterson, C. L., Kruger, W. and Herskowitz, I. (1991). A functional interaction between the C-terminal domain of RNA polymerase II and the negative regulator SIN1. *Cell* **64**, 1135-1143.

Petesch, S. J. and Lis, J. T. (2012). Overcoming the nucleosome barrier during transcript elongation. *Trends Genet.* **28**, 285-294.

Ray-Gallet, D., Woolfe, A., Vassias, I., Pellentz, C., Lacoste, N., Puri, A., Schultz, D. C., Pchelintsev, N. A., Adams, P. D., Jansen, L. E. et al. (2011). Dynamics of histone H3 deposition in vivo reveal a nucleosome gap-filling mechanism for H3.3 to maintain chromatin integrity. *Mol. Cell* **44**, 928-941.

Santoro, R. and Grummt, I. (2005). Epigenetic mechanism of rRNA gene silencing: temporal order of NoRC-mediated histone modification, chromatin remodeling, and DNA methylation. *Mol. Cell. Biol.* **25**, 2539-2546.

Saunders, A., Werner, J., Andrulis, E. D., Nakayama, T., Hirose, S., Reinberg, D. and Lis, J. T. (2003). Tracking FACT and the RNA polymerase II elongation complex through chromatin in vivo. *Science* **301**, 1094-1096.

Schwabish, M. A. and Struhl, K. (2006). Asf1 mediates histone eviction and deposition during elongation by RNA polymerase II. *Mol. Cell* **22**, 415-422.

Singh, J. and Padgett, R. A. (2009). Rates of in situ transcription and splicing in large human genes. *Nat. Struct. Mol. Biol.* **16**, 1128-1133.

Snodgrass, R. G., Collier, A. C., Coon, A. E. and Pritsos, C. A. (2010). Mitomycin C inhibits ribosomal RNA: a novel cytotoxic mechanism for bioreductive drugs. *J. Biol. Chem.* **285**, 19068-19075.

Sternberg, P. W., Stern, M. J., Clark, I. and Herskowitz, I. (1987). Activation of the yeast HO gene by release from multiple negative controls. *Cell* **48**, 567-577.

Strohner, R., Németh, A., Nightingale, K. P., Grummt, I., Becker, P. B. and Längst, G. (2004). Recruitment of the nucleolar remodeling complex NoRC establishes ribosomal DNA silencing in chromatin. *Mol. Cell. Biol.* **24**, 1791-1798.

Studitsky, V. M., Clark, D. J. and Felsenfeld, G. (1994). A histone octamer can step around a transcribing polymerase without leaving the template. *Cell* **76**, 371-382.

Studitsky, V. M., Clark, D. J. and Felsenfeld, G. (1995). Overcoming a nucleosomal barrier to transcription. *Cell* **83**, 19-27.

Studitsky, V. M., Kassavetis, G. A., Geiduschek, E. P. and Felsenfeld, G. (1997). Mechanism of transcription through the nucleosome by eukaryotic RNA polymerase. *Science* **278**, 1960-1963.

Tachiwana, H., Kagawa, W., Osakabe, A., Kawaguchi, K., Shiga, T., Hayashi-Takanaka, Y., Kimura, H. and Kurumizaka, H. (2010). Structural basis of instability of the nucleosome containing a testis-specific histone variant, human H3T. *Proc. Natl. Acad. Sci. USA* **107**, 10454-10459.

Tanaka, Y., Tawaramoto-Sasanuma, M., Kawaguchi, S., Ohta, T., Yoda, K., Kurumizaka, H. and Yokoyama, S. (2004). Expression and purification of recombinant human histones. *Methods* **33**, 3-11.

Thebault, P., Boutin, G., Bhat, W., Rufiange, A., Martens, J. and Nourani, A. (2011). Transcription regulation by the noncoding RNA SRG1 requires Spt2-dependent chromatin deposition in the wake of RNA polymerase II. *Mol. Cell. Biol.* **31**, 1288-1300.

Vintermist, A., Böhm, S., Sadeghifar, F., Louvet, E., Mansén, A., Percipalle, P. and Östlund Farrants, A.-K. (2011). The chromatin remodelling complex B-WICH changes the chromatin structure and recruits histone acetyl-transferases to active rRNA genes. *PLoS ONE* **6**, e19184.

Wang, H., Walsh, S. T. R. and Parthun, M. R. (2008). Expanded binding specificity of the human histone chaperone NASP. *Nucleic Acids Res.* **36**, 5763-5772.

Ward, G. K., Shihab-el-Deen, A., Zannis-Hadjopoulos, M. and Price, G. B. (1991). DNA cruciforms and the nuclear supporting structure. *Exp. Cell Res.* **195**, 92-98.

Winkler, D. D. and Luger, K. (2011). The histone chaperone FACT: structural insights and mechanisms for nucleosome reorganization. *J. Biol. Chem.* **286**, 18369-18374.

Winston, F., Chaleff, D. T., Valent, B. and Fink, G. R. (1984). Mutations affecting Ty-mediated expression of the HIS4 gene of Saccharomyces cerevisiae. *Genetics* **107**, 179-197.

Wolffe, A. (1998). *Chromatin: Structure and Function*, 3rd edn. San Diego, CA: Academic Press.

Xiao, H., Jackson, V. and Lei, M. (2006). The FK506-binding protein, Fpr4, is an acidic histone chaperone. *FEBS Lett.* **580**, 4357-4364.

Zentner, G. E., Saiakhova, A., Manaenkov, P., Adams, M. D. and Scacheri, P. C. (2011). Integrative genomic analysis of human ribosomal DNA. *Nucleic Acids Res.* **39**, 4949-4960.